Degago, S. A. *et al.* (2011). *Géotechnique* **61**, No. 10, 897–908 [http://dx.doi.org/10.1680/geot.9.P.112]

Use and misuse of the isotache concept with respect to creep hypotheses A and B

S. A. DEGAGO*, G. GRIMSTAD†, H. P. JOSTAD*†, S. NORDAL* and M. OLSSON‡

Time-dependent settlements of thick in situ clay layers are normally analysed based on results of thin laboratory specimens. However, the time used to complete primary consolidation is significantly different for laboratory specimens and in situ soil layers. Two totally different cases, referred to as creep hypotheses A and B, have been used as a basis of discussion to assess the effect of creep during the primary consolidation phase. Several laboratory and field experiments have been conducted to study the effect of soil layer thickness on the time-dependent compressibility of a soil layer. Some of these tests seemed to support hypothesis A, others hypothesis B, and in some cases showed a behaviour between the two. As a result this question has continued to be a controversial topic among researchers, and remains to be an issue that needs to be resolved. In this study, some relevant experimental investigations from the literature are thoroughly studied and critically reviewed, and also explained consistently using the isotache concept. This work indicates that the isotache approach can capture the main characteristics of the time-dependent compressibility of clays during both the primary and secondary consolidation phases. It is also shown that the misuse of the isotache concept, as reported in the literature, may give a confusing picture of reality. Based on the considered data, it is demonstrated that the measured time-dependent compressibility of clays agrees well with hypothesis B.

KEYWORDS: clays; compressibility; consolidation; creep; deformation; settlement

Les tassements en fonction du temps d'épaisses couches d'argile in situ sont normalement analysés sur la base de spécimens de laboratoire de faible épaisseur. Toutefois, les délais nécessaires pour la réalisation de la consolidation primaire sont sensiblement différents pour les spécimens de laboratoire et les couches de sol in situ. On a utilisé deux cas totalement différents, désignés hypothèses de glissement A et B, comme éléments de base pour des discussions, dont le but était d'établir l'effet du glissement au cours de la phase de consolidation primaire. On a effectué plusieurs expériences en laboratoire et sur le terrain afin d'étudier l'effet de l'épaisseur des couches de sol sur la compressibilité en fonction du temps de la couche de sol. Certains de ces tests semblent favoriser l'hypothèse A, d'autres l'hypothèse B, et, dans certains cas, un comportement situé entre les deux. En conséquence, ce problème reste une question controversée entre les chercheurs, ainsi qu'un problème à résoudre. Dans la présente étude, on procède à une étude approfondie ainsi qu'à l'examen critique de certaines recherches expérimentales pertinentes dans des ouvrages sur cette question, que l'on explique logiquement en appliquant le concept des isotaches. La présente communication indique que le principe des isotaches permet de saisir les principales caractéristiques de la compressibilité des argiles en phase de consolidation primaire et secondaire. Elle indique également que l'application erronée du concept de l'isotache, décrit dans des ouvrages, risque de fausser la réalité des choses. Sur la base des données examinées, on démontre que la compressibilité des argiles mesurée en fonction du temps est en parfait accord avec l'hypothèse B.

INTRODUCTION

The settlement behaviour of in situ soft soil layers is normally studied based on test results deduced from laboratory specimens. In geotechnical practice, standard oedometer and triaxial tests are usually conducted to study soil deformation as a response to an applied action of stress and time. Laboratory specimens are subjected to loading that reproduces the action of stress in the field; however, reproducing the action of time is not easy, since significantly different timescales are involved. Still, time-dependent settlements of thick in situ soft soil layers are usually analysed based on experimental results derived from thin laboratory specimens. The time duration to complete primary consolidation is considered to be an important difference between laboratory specimens and in situ soil layers. In the laboratory, consolidation may last for the order of minutes, whereas in thick in situ clay layers the consolidation period could be of the order of several decades (Larsson & Mattsson, 2003; Leroueil, 2006). Therefore, in order to achieve acceptable field predictions, it is very important to understand the time-scaling effect between a thin laboratory specimen and a thick in situ soil layer. How to extrapolate the time-dependent behaviour of clays from fast laboratory tests towards slow field condition has been a topic of active debate among researchers (Mesri, 2003; Leroueil, 2006). This paper aims to clarify the controversies related to scale effects, based on a critical review of laboratory tests from the literature, supported by illustrative numerical analyses.

Manuscript received 12 September 2009; revised manuscript accepted 15 October 2010. Published online ahead of print 22 February 2011. Discussion on this paper closes on 1 March 2012, for further details see p. ii.

* Norwegian University of Science and Technology, Trondheim, Norway.
† Norwegian Geotechnical Institute, Oslo, Norway.
‡ Chalmers University of Technology, Gothenburg, and Swedish Geotechnical Institute, Gothenburg, Sweden.

BACKGROUND

In their state-of-the art report, Ladd *et al.* (1977) raised an important question related to creep during primary consolidation. The fundamental question was: 'Does creep act as a separate phenomenon while excess pore pressures dissipate during primary consolidation?' If it does, then for a given effective vertical stress increment the end-of-primary (EOP) vertical strain depends upon the duration of primary

consolidation, and hence on the thickness of the consolidating soil layer. Such a consideration led to the realisation of two possible extreme effects of sample thickness, which are summarised in Fig. 1 in terms of hypotheses A and B. In hypothesis A, the strain at EOP is assumed to be independent of the consolidation period, whereas hypothesis B predicts an increasing EOP strain with increasing consolidation period or increasing sample thickness.

A possible implication of the two creep hypotheses in terms of effective stress–void ratio (strain) is stated as follows. Hypothesis A predicts that the relationship between EOP void ratio (strain) and effective stress is the same for both laboratory and field conditions. This means that the EOP preconsolidation stress is identical for laboratory specimens and in the in situ condition. Hypothesis B yields a relationship between an in situ EOP strain and effective stress that is different from the corresponding laboratory curve, such that the in situ EOP preconsolidation stress is lower than that determined from an EOP laboratory test. Admitting that Ladd *et al.* (1977) were themselves biased towards hypothesis A, they conclude that 'Little definitive data exists to show which of the two hypotheses is more nearly correct for the majority of cohesive soils.' Since 1977, this concern has continued to be a topic of active discussion among researchers, and remains an issue that needs to be resolved. A summary of some of the discussions can be found in Mesri (2003) and Leroueil (2006).

Early work by researchers studying creep (Šuklje, 1957; Bjerrum, 1967; Janbu, 1969; Šuklje, 1969) assumed that the creep rate was given by the current effective stress and the current void ratio (strain). In other words, any combination of void ratio (strain), effective stress and rate of change of void ratio (strain rate) is considered to be unique throughout the primary and secondary consolidation phases. These formulations can be classified as isotache models, and imply hypothesis B. Such approaches have been advocated and used as a basis for further research developments that consider creep during primary consolidation (e.g. Svanø *et al.*, 1991; Kutter & Sathialingam, 1992; Den Haan, 1996; Stolle *et al.*, 1999; Vermeer & Neher, 1999; Kim & Leroueil, 2001; Nash & Ryde, 2001; Yin *et al.*, 2002; Imai *et al.*, 2003; Leroueil, 2006; Laloui *et al.*, 2008; Leoni *et al.*, 2008; Watabe *et al.*, 2008b; Grimstad & Degago, 2010; Grimstad *et al.*, 2010; Karim *et al.*, 2010; Nash, 2010). Other researchers, supporting hypothesis A, found experimentally that the EOP void ratio seemed to be independent of the consolidation period (Mesri & Godlewski, 1979; Choi, 1982; Mesri & Choi, 1985; Feng, 1991; Mesri, 2003; Mesri & Vardhanabhuti, 2006; Mesri, 2009). This group of researchers also advocate the existence of creep during primary consolidation, but they believed that the role of creep is controlled by total strain rate as a function of stress state and effective stress rate, indicating that there is no unique relationship among effective stress, strain and strain rate during primary consolidation (Mesri, 1990; Feng, 1991; Mesri *et al.*, 1995; Mesri, 2009). Their argument can be elaborated by the subsequent statements: soil compression is caused by two interrelated contributions, which are due to change in effective stress (stress compressibility) and change in time (time compressibility). It is assumed that the combination of these two interrelated components varies according to the effective stress rate and the duration of primary consolidation. Hence the difference in effective stress rate and consolidation duration that exists between thin and thick soil layers is claimed to govern the contribution of the stress and time compressibility components to yield an EOP void ratio (strain) that is independent of the consolidation period.

Several laboratory and field experiments have been conducted to investigate the effects of layer thickness on the compressibility of clayey soils (Berre & Iversen, 1972; Aboshi, 1973; Felix, 1979; Aboshi *et al.*, 1981; Choi, 1982; Mesri & Choi, 1985; Kabbaj *et al.*, 1988; Feng, 1991; Imai & Tang, 1992; Tsukada & Yasuhara, 1995; Chih-Hao, 2002; Li *et al.*, 2004; Tanaka, 2005; Konovalov & Bezvolev, 2005; Watabe *et al.*, 2008a, 2009; Degago *et al.*, 2010). Most of these tests have been conducted to examine the two creep hypotheses and, as a consequence, have played a significant role in advocating them. In this paper, laboratory investigations that focused on assessing the creep contribution during primary consolidation are thoroughly studied and critically reviewed, along with the support of illustrative numerical analyses. The numerical model used in the analyses is based on the isotache concept, which is described in the next section.

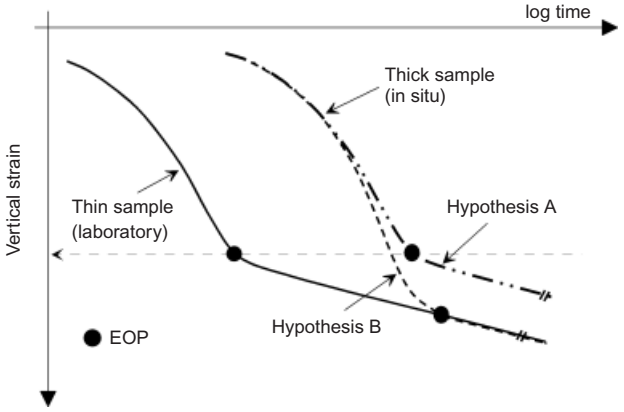

Fig. 1. Effect of sample thickness according to creep hypotheses A and B (after Ladd *et al.*, 1977). Note: same $\Delta\sigma'/\sigma'_{v0}$ for both samples

THE ISOTACHE CONCEPT

The isotache concept was originally proposed by Šuklje (1957) in order to describe rate effects on the compressibility of clayey soils. This approach states that the rate of change of void ratio is given by the prevailing void ratio and effective stress.

The concept of isotaches can be illustrated using the sketch shown in Fig. 2. The series of parallel broken lines in the figure are creep isotaches. Each creep isotache corresponds to a constant void ratio rate, $\dot{e}_{j+n}$. This means that any combination of void ratio, vertical effective stress and rate of change of void ratio is unique, and this remains valid during the entire soil compression process (primary and secondary consolidation phases). For instance, consider a soil element close to a draining boundary. The initial state of this soil element is assumed to be given by point A. A vertical total stress increment, $\Delta\sigma'_v$, is then applied and left to creep for some time. The path followed is represented by the solid line ABCDE. This path is dependent on the distance of the soil element from the drainage boundary, as the effective stress rate and strain rate are governed by the consolidation process. Depending on the duration of the applied effective stress, the final state of the soil element can be B, C, D or E.

In this paper, the isotache concept is used to provide numerical illustrations. These simulation results are used to demonstrate the implications of the isotache approach. Two types of idealised case are considered. The first case demonstrates the compressibility characteristics of two different specimen thicknesses. The second case shows the local compressibility of soil elements within a thick specimen, but

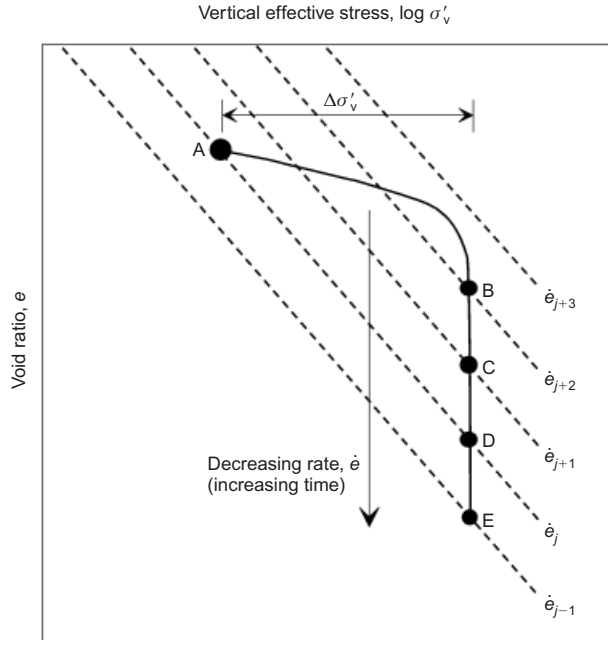

Fig. 2. Illustration of the isotache concept

located at different distances from the drainage boundary. The finite-element code PLAXIS (2D version 9) with the soft soil creep (SSC) model (Stolle *et al.*, 1999; Vermeer & Neher, 1999) was utilised in the numerical simulations. Even though SSC is used in this study, it must be acknowledged that there are several models based on the isotache concept that produce essentially similar results.

CASE I: COMPRESSIBILITY OF SPECIMENS WITH DIFFERENT THICKNESSES

Description of simulation

Two idealised specimens with thicknesses of 1 cm and 10 cm were simulated in a uniaxial strain condition with drainage at the top. The loading and drainage conditions were defined to resemble oedometer conditions. Both specimens were initially prestressed to $\sigma'_v = 10$ kPa, $\sigma'_h = 5{\cdot}2$ kPa. The initial preconsolidation stress, p'_c, was specified to be 100 kPa. This p'_c value corresponds to a preconsolidation stress obtained in a test of one day's duration, between each load increment, in an incremental oedometer test. A standard incremental oedometer loading scheme was adopted with applied vertical stresses of 25 kPa (a vertical stress increment of 15 kPa), 50 kPa, 100 kPa, 200 kPa, 400 kPa, 700 kPa, 1200 kPa and 2000 kPa. For the EOP oedometer test simulations, the incremental load duration lasted until 99% of the initial excess pore pressure increment had dissipated. The soil parameters adopted for the simulations are listed in Table 1. The definitions of the SSC compressibility parameters, in isotropic compression, are illustrated in Fig. 3 in terms of volumetric strain ε_v, mean effective stress p' and time t. The SSC model uses a shape parameter M that controls the steepness of the cap. In this paper, the parameter M was chosen such that it is determined based on the coefficient of earth pressure under virgin loading (K_0^{NC}) considerations (for further details see the PLAXIS user's manual).

Table 1. Soil properties adopted for the oedometer simulations

Soil parameter	Value
Permeability, k: m/s	5×10^{-9}
Earth pressure coefficient under virgin loading, K_0^{NC}	0·52
Modified swelling index, κ^*	0·021
Modified compression index, λ^*	0·091
Modified creep index, μ^*	0·0033
Friction angle, ϕ: degrees	30
Poisson's ratio for unloading–reloading: ν_{ur}	0·15

Simulation results of idealised case I

Standard EOP simulations. Standard incremental oedometer test schemes were simulated under EOP conditions for the thin (1 cm) and thick (10 cm) specimens. The axial deformation at the top of the specimens, δ_v, was normalised by the respective initial height, h_i. This gives a strain measure that will be referred to in this paper as a nominal strain.

The curved lines in Fig. 4 show vertical strain, ε_v, against the effective stress history path followed by a soil element close to the top of each specimen. The end points at each of the stress increments mark the final EOP state of the specimens. When these EOP points are connected for a stress state above the initial p'_c, they define an isotache corresponding to the rate at EOP consolidation. Hence, when the EOP points are connected, they define a reference isotache that corresponds to an EOP strain rate (in Fig. 4, the symbols with a dot on top are used to identify the creep isotaches corresponding to the 1 cm and 10 cm thick specimen). For a load increment that takes place in a stress regime well before reaching p'_c, the behaviour of both the thin and thick specimens is strongly influenced by elasticity, and the contribution from creep is insignificant. Hence both specimens follow the same path until they approach the initial preconsolidation stress, p'_c. However, while approaching the initial p'_c, differences start to arise as strain rate effects come into play. It is also seen that the thick specimen yields at a lower effective stress than the thin specimen. The difference in the EOP nominal strain remains constant during the normally consolidated regime. This also means that the incremental EOP nominal strains of the two speci-

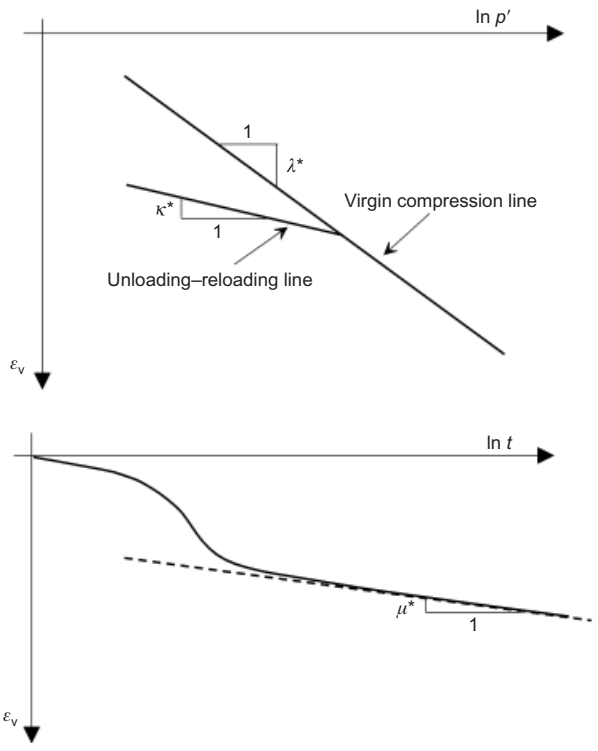

Fig. 3. Definition of SSC parameters (PLAXIS user's manual)

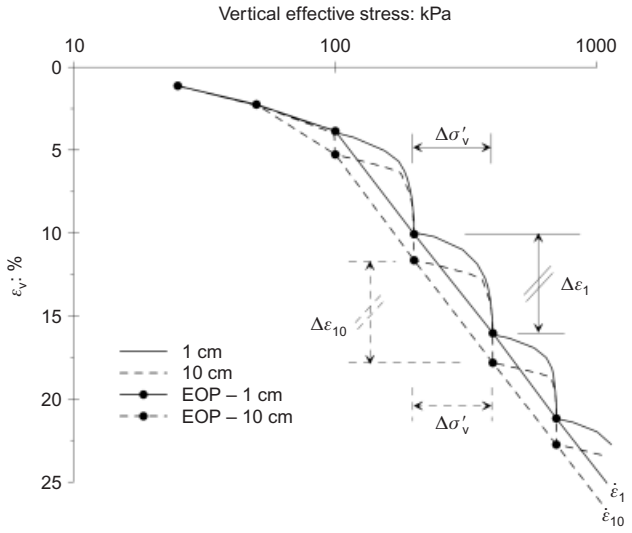

Fig. 4. EOP paths followed by soil element close to top of specimens (curved lines) and isotache lines corresponding to EOP state of specimens (straight lines)

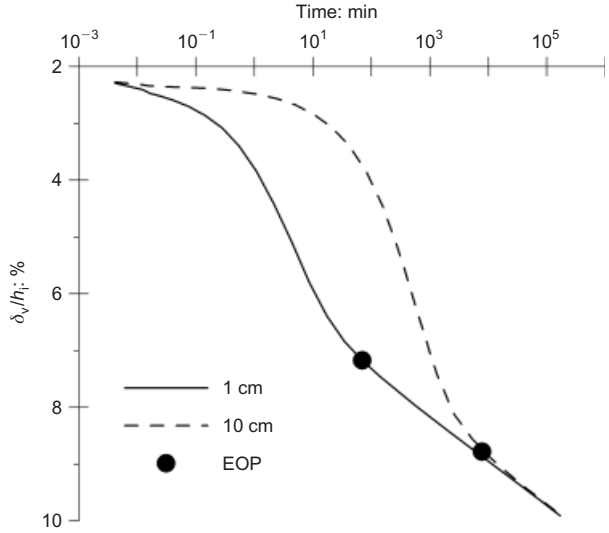

Fig. 5. Load increment from 50 to 150 kPa exceeding initial $p'_c = 100$ kPa

mens become practically equal for effective stress increments in the normally consolidated regime. What actually happens, in Fig. 4, can be further elaborated by considering the interplay between the creep rate and the corresponding consolidation period. Before the initial p'_c, both specimens have a similar creep rate. During an effective stress increment that exceeds the initial p'_c, the consolidation periods will be significantly different for the two specimens, and this leads to different EOP strains. However, for stress increments in the normally consolidated regime, the thin specimen deforms with a higher creep rate for a shorter consolidation period, whereas the thick specimen deforms with a lower creep rate for a longer consolidation period. Consequently, the incremental EOP strains, in the normally consolidated regime, will be almost the same for both specimens.

The overall picture of the EOP consolidation process of the thin and thick specimens is presented in Fig. 4. The next step is to take a closer look at the effect of creep at different effective stresses in reference to the initial preconsolidation stress, p'_c. Consolidation behaviour that takes place well before approaching the initial p'_c is not interesting, as no distinction can be made between the thin and thick specimens. However, the consolidation behaviours close to p'_c and after exceeding the initial p'_c are investigated in separate simulations.

Load increment that exceeds the initial preconsolidation stress, p'_c. To study the creep phenomenon while exceeding the initial p'_c, both specimens were incrementally loaded following a standard loading procedure, with an EOP condition, up to 50 kPa. This ensured that both specimens were in an overconsolidated state regime, and that the test simulations therefore started at the same effective stress–nominal strain or effective stress–void ratio state. Subsequently an additional load increment of 100 kPa was applied such that the initial $p'_c = 100$ kPa was exceeded. Afterwards, both specimens were left to creep at 150 kPa for 100 days. Fig. 5 shows that both specimens essentially start at the same point but end up having different EOP nominal strains. The EOP nominal strain is larger for the thick specimen. However, after a long time, the nominal strain–time curves of the thin and thick specimens converge to the same line.

Load increment immediately after exceeding initial preconsolidation stress, p'_c. To study the settlement characteristics at the beginning of the virgin stress regime, both specimens were incrementally loaded following a standard loading procedure, with an EOP condition, up to 200 kPa. This ensured that the initial $p'_c = 100$ kPa was exceeded. Afterwards, both specimens were allowed to creep for 100 days under 200 kPa. The results are presented in two ways as shown in Figs 6(a) and 6(b). When the specimens reach the initial p'_c at 100 kPa the void ratios (nominal strains) become different, and this defines the starting state for the next stress increment. When an additional 100 kPa increment is applied, giving a total stress of 200 kPa, both specimens yield a different EOP void ratio, that increases with specimen thickness. After creeping for a longer duration at 200 kPa, the deformation–time curves of the two specimens converge to the same line, as shown in Fig. 6(a). However, the calculated results can also be presented in a different way, as shown in Fig. 6(b). In this case only the changes in the nominal strain within the actual load increment are presented. It is observed that the EOP nominal strain increments are closer to each other, and show only a slight tendency to increase with the greater thickness. This is because the effect of exceeding the initial p'_c is pronounced to some extent. The final parts of these curves are parallel, and will never converge to the same line.

Load increment long after exceeding initial preconsolidation stress, p'_c. The aim of this simulation is to study the deformations at a stress level that is sufficiently greater than the initial p'_c. Hence both specimens were incrementally loaded following a standard EOP loading procedure up to 400 kPa, and left to creep for 100 days at this stress level. The results of this simulation are presented in Figs 7(a) and 7(b). The shapes of the curves are very similar to the shapes obtained when the samples were loaded from 100 kPa to 200 kPa. However, the slight tendency of the EOP incremental nominal strain to increase with sample thickness observed at 200 kPa (see Fig. 6(b)) is not observed when the specimens are loaded from 200 kPa to 400 kPa (Fig. 7(b)). The main reason is that the effect of exceeding the initial p'_c of 100 kPa does not affect the incremental nominal strains for the load increment between 200 and 400 kPa. This means that the EOP incremental nominal strains are almost identical

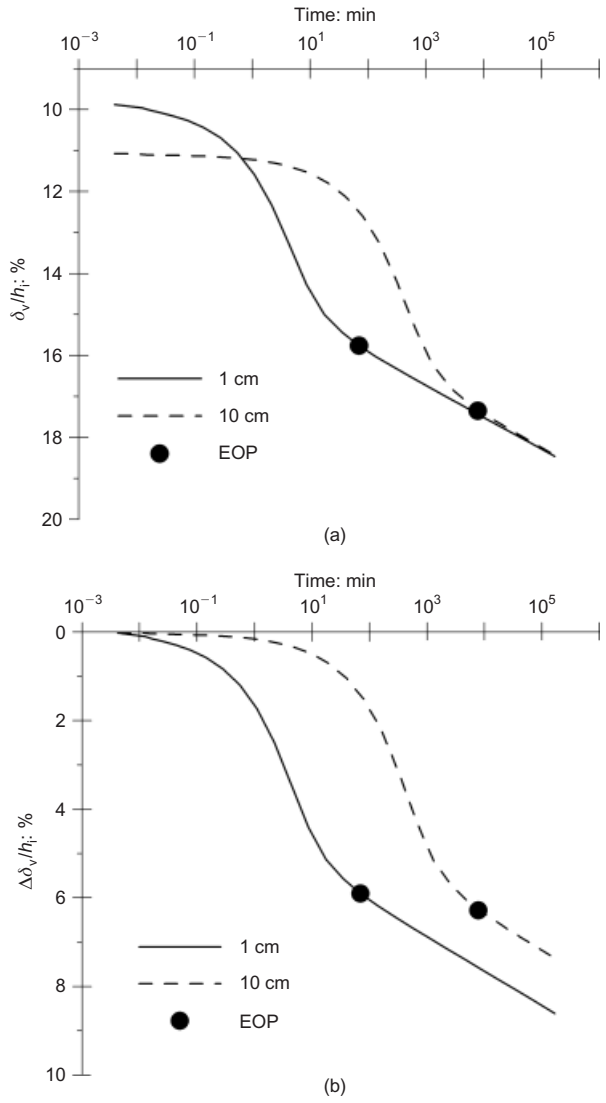

Fig. 6. Load increment from 100 to 200 kPa in terms of: (a) absolute nominal strains; (b) incremental nominal strains. Allowed to creep after EOP at 200 kPa

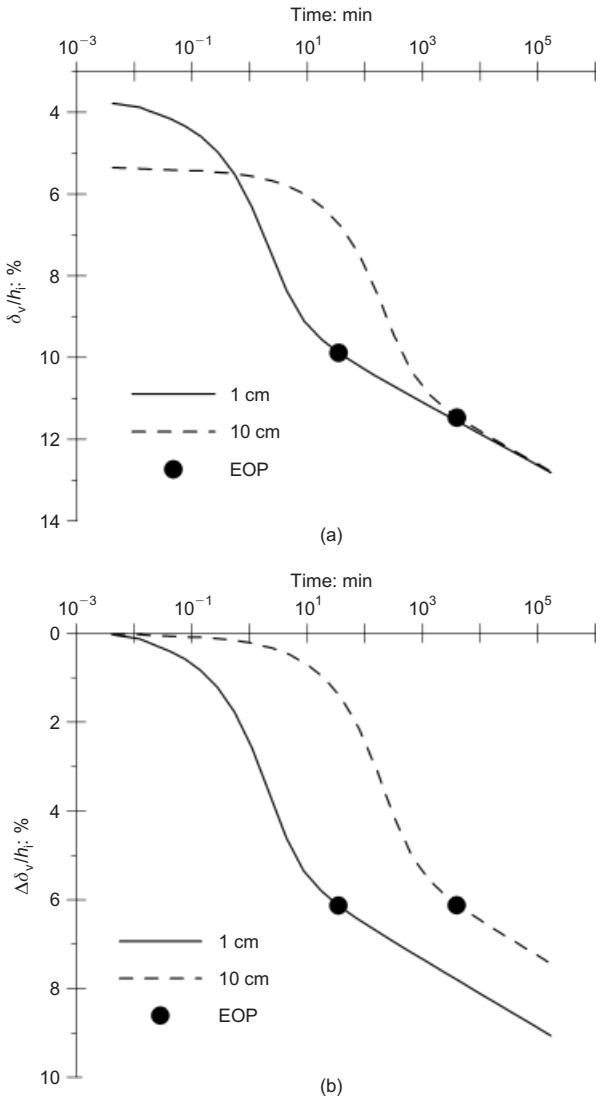

Fig. 7. Load increment from 200 to 400 kPa in terms of: (a) absolute nominal strains; (b) incremental nominal strains. Allowed to creep after EOP at 400 kPa

for the thin and thick specimen when the load increment is sufficiently above the initial p'_c.

Literature review of EOP experiments on specimens of different thicknesses

The results from the idealised cases presented in the previous section will be used critically to discuss previously conducted EOP experiments on specimens of varying thickness. The tests reviewed are discussed in chronological order. The experiment conducted by Feng (1991) and Choi (1982) on specimens 127 and 508 mm thick, which were used to advocate hypothesis A, are addressed in a separate paper (Degago *et al.*, 2009) and will not be discussed here. However, it is worthwhile mentioning that Degago *et al.* (2009) have shown that re-interpretation of these tests, for consistent EOP criteria, yields results that support hypothesis B. In addition, these test observations were compared with numerical simulations using an isotache model that gave results that fit very well with the measurements.

Experiment by Aboshi (1973). Aboshi (1973) conducted a series of carefully designed laboratory and field tests with varying specimen sizes. The investigated soil was reconstituted sedimentary marine clay from Hiroshima Bay. In order to avoid the effects of friction and stress distribution on the side walls, all the tests had similar diameter (d) to height (h) ratios given by $d/h = 3$. In addition, silicone oil was used to avoid possible side friction. Three different heights, 2, 4·8 and 20 cm, were tested in the laboratory, whereas another two heights, 40 and 100 cm, were tested in the field.

A preliminary consolidation stage up to 20 kPa, which is necessary to perform the test in a normally consolidated regime, was limited in time by the end of primary consolidation. Afterwards settlements of long duration were conducted by one loading step from 20 to 80 kPa. The incremental EOP nominal strains for specimen heights of 2, 4·8, 20, 40 and 100 cm were respectively approximated as 7·3%, 7·4%, 8·2%, 7·8% and 8·4% using Taylor's graphical construction, and 8·25%, 8·2%, 8·3%, 8·35% and 8·9% using Casagrande's graphical construction (Choi, 1982; Oka, 2005).

The experiments conducted by Aboshi (1973) have been widely discussed by various researchers (see below), and were perceived differently. Aboshi (1973) concluded that the observed soil behaviour deviates from the isotache theory, proposed by Šuklje (1957), because the measured settlement curves tend to be parallel instead of converging to one line. Choi (1982) and Mesri (2009) re-interpreted the EOP nominal strains to show that they are more or less similar to

each other. Mesri & Choi (1985) and Mesri (2009) argued that the observed range of EOP strains for different thicknesses is in agreement with hypothesis A, and the observed small variations could be due to issues related to possible problems linked to single lead increment tests. These test results (see Fig. 8) have also been claimed to show that the real soil behaviour lies in between hypotheses A and B (Yasuhara, 1982; Leroueil *et al.*, 1985; Imai & Tang, 1992; Hawlader *et al.*, 2003; Li *et al.*, 2004; Watabe *et al.*, 2009). Oka (Oka *et al.*, 1986; Oka, 2005) described Aboshi's observation as hypothesis C (a hypothesis between A and B), and proposed a numerical procedure that simulates the possible creep hypotheses A, B and C.

The authors' view on these experiments is presented as follows. Soil specimens of Hiroshima Bay with different thicknesses were reconstituted for different durations with an increasing time for an increasing specimen thickness. The results of the actual stress increment (20 to 80 kPa) were presented in terms of incremental nominal strains against time. These tests were conducted after exceeding the initial p'_c. Hence they correspond to the idealised case shown in Fig. 6(b). The slight increase in the incremental EOP nominal strain with increasing specimen thickness can also be seen both in the experiment and in the simulated idealised case.

When the isotache concept was first presented (Šuklje, 1957), it was meant to describe the compressibility of soils subjected to long-term creep, such that the primary consolidation phase plays a minor role in the whole compression process. The consequence of this is that the time–settlement curves of thick and thin specimens converge to the same line or void ratio. Hence the next stress increment will start at the same void ratio, irrespective of the thickness or stress history, and the time–settlement curves again converge to the same line and so on, analogous to Fig. 5. Aboshi (1973) originally presented the experimental results in Fig. 6(b) format, and compared them with a set of isotaches plotted in Fig. 6(a) format. In other words, the experiments were plotted in terms of change in nominal strain, but they were compared against a set of isotaches valid for total nominal strains. As a consequence, Aboshi wrongly concluded that

> the creep settlement curves of every tests become almost parallel in their final stages. However these creep settlement curves do not coincide in one line on the creep curve of standard oedometer test, as shown in Šuklje's isotaches theory.

The main observation can be summarised as follows. There is a slight tendency for the EOP nominal strain increment to increase with increasing thickness. This agrees with simulation results of the idealised case where the load step exceeds the initial p'_c, as shown in Fig. 6(b). The effect of increasing EOP nominal strain with thickness, as implied by hypothesis B, would have been significantly larger if the experimental results were presented for the whole stress history in terms of the absolute nominal strain or void ratio.

Experiment by Imai & Tang (1992). Imai & Tang (1992) developed a system of interconnected consolidometers, and carefully conducted a series of experiments on a marine clay from Yokohama Bay. The tested material was carefully reconstituted such that the desired uniformity of the soil was maintained. Each sub-specimen had a thickness of 0·5 cm and a diameter of 6 cm. Special measures were also taken to minimise possible errors that could arise from such thin specimens.

Prior to the main experiment, each thin specimen was preconsolidated to an effective vertical stress of 39·2 kPa. A set of EOP tests were conducted using the interconnected system, such that incremental loads were applied until 99% of the initial excess pore pressure was dissipated. The initial total specimen thicknesses studied under EOP conditions were 1, 2 and 4 cm.

The results of the last load increment, from 156·8 kPa to 313·6 kPa, are shown in Fig. 9, and were used by Imai & Tang to verify hypothesis A. These results correspond to the idealised case illustrated in Fig. 7(b). The reason why the experiments seem to agree with hypothesis A is that they are presented in terms of change in void ratio, and the stress range is far above the initial p'_c. It is worth mentioning that Imai & Tang have conducted another set of experiments to illustrate the possibility of obtaining results in accordance with hypothesis B. To achieve this, they let their thin and thick specimens creep for the same duration of 24 h, and then studied the EOP void ratio that resulted from the next load increment. This test procedure is not a true EOP test, as neither of the specimens started from its respective EOP states. Verification of hypothesis B using these results was considered to be incorrect and misleading according to Mesri (2003), as the comparison lacks consistency in EOP procedure. However, had Imai & Tang (1992) presented their

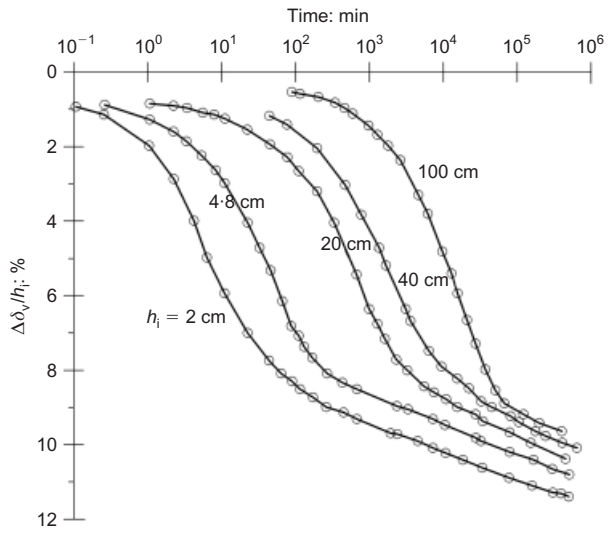

Fig. 8. Results of consolidation test on samples of different thickness (after Aboshi, 1973)

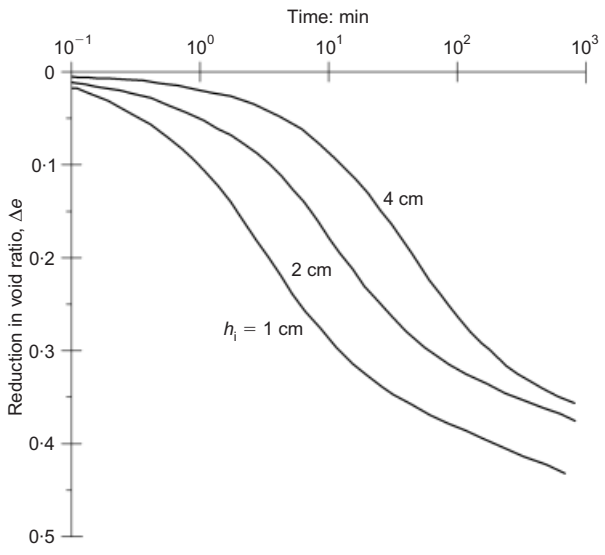

Fig. 9. Experimental results for specimens of different thickness during last loading increment (after Imai & Tang, 1992)

EOP test results (Fig. 9) in terms of absolute void ratio, rather than change in void ratio, they would have verified hypothesis B without even the need to do another experiment with an inconsistent EOP procedure.

Experiment by Konovalov & Bezvolev (2005). Konovalov & Bezvolev (2005) conducted EOP consolidation tests on natural clayey soil originating from a post-glacial marine lithorine deposit. A specially designed consolidometer was used to test specimens with a diameter of 5·5 cm, and with the possibility of varying the specimen thickness within the range 1–10 cm. The consolidometer used an impenetrable rubber jacket and incompressible confined liquid to avoid the possibility of friction along the lateral surface of the samples. This was considered to be important to control the uniformity of the test specimens.

The test specimens were reconsolidated back to their in situ state, depicted by an effective stress of 30 kPa. Subsequent to reconsolidation, the test specimens were subjected to a stepped loading for a duration defined by 95% dissipation of the initial excess pore pressure. After reaching an effective stress level of 230 kPa using this EOP loading procedure, the specimens were subjected to an additional stress increment of 200 kPa and left to creep for more than 70 days.

Figure 10 shows the results of the last load increment (230 to 430 kPa) in two ways, as originally presented by Konovalov & Bezvolev (2005). These results support the isotache concept as shown in Figs 7(a) and 7(b). The experiments demonstrated that disregarding the effect of the void ratio–stress history of a soil has the consequence of giving a confusing picture of reality.

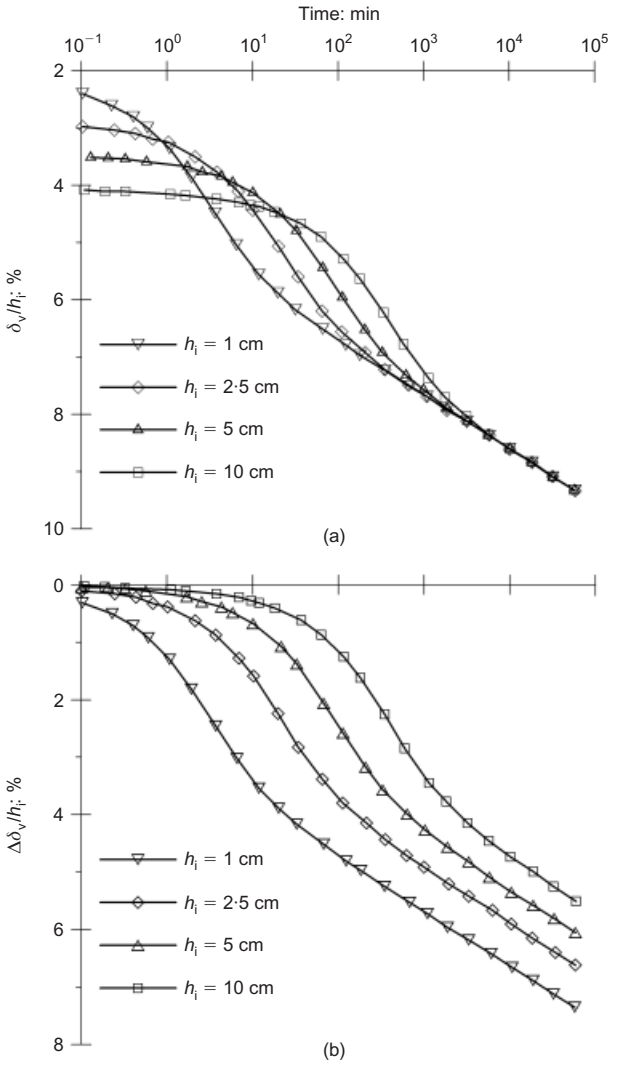

Fig. 10. Consolidation curves for load increment from 230 to 430 kPa in terms of (a) overall nominal strain; (b) incremental nominal strains (after Konovalov & Bezvolev, 2005)

CASE II: LOCAL COMPRESSIBILITY OF SOIL ELEMENTS WITHIN A SPECIMEN

Description of the simulation

In this idealised case, the isotache principles are illustrated by considering the local compressibility of soil elements within a specimen. The behaviours of soil elements located at different distances from a drainage boundary are studied for three different stress regimes in reference to the initial p'_c.

A 50 cm thick soil specimen with a diameter of 6·35 cm was studied under isotropic triaxial loading and one-way drainage conditions. A very fine mesh of 15 node elements was adopted under axisymmetric condition. The soil was considered to have an initial preconsolidation stress, p'_c, of 74 kPa, corresponding to a test of one day's duration, between each load increment, in an incremental oedometer test. An incremental loading scheme was adopted with applied isotropic stresses, σ_c, of 14 kPa, 28 kPa, 41 kPa, 62 kPa, 83 kPa and 125 kPa. The loading stages were adopted from a similitude experiment conducted by Feng (1991). All stress increments were applied instantaneously and kept constant until 95% dissipation of the initial excess pore pressure was achieved. The soil parameters adopted for the SCC model are listed in Table 2. These soil parameters represent the Batiscan clay, as reported by Feng (1991). The geometry of the finite-element model is shown in Fig. 11.

Table 2. Soil parameters adopted for isotropic triaxial simulations based on Feng (1991)

Soil parameter	Value
Permeability, k_v: m/day	$6 \times 10-5$
Earth pressure coefficient under virgin loading, K_0^{NC}	0·60
Change of permeability, c_k	1·10
Initial void ratio, e_0	2·25
Modified swelling index, κ^*	0·0084
Modified compression index, λ^*	0·189
Modified creep index, μ^*	0·0059
Friction angle, ϕ: degrees	30
Poisson's ratio for unloading–reloading, ν_{ur}	0·15

Simulation results

Deformation responses were studied at points 1, 2, 3 and 4 (shown in Fig. 11), which divide the thick specimen into equal sections of four 12·5 cm high sub-specimens. The incremental axial compressions of each sub-specimen, $\Delta\delta_v$, are normalised by the initial sub-specimen height, h_i, of 12·5 cm and they are presented for the three different stress regimes with reference to the initial p'_c. Before and after exceeding the initial p'_c, simulation results (Fig. 12(a) and (c)) showed that the incremental deformation–time curves of the four sub-specimens came to the same point at the EOP state. Nevertheless, the same set of curves will never come to the same point at the EOP state for a stress increment that exceeds the initial p'_c (Fig. 12(b)). However, if the whole specimen is left to creep for a very long time after the EOP state, such that the consolidation period becomes

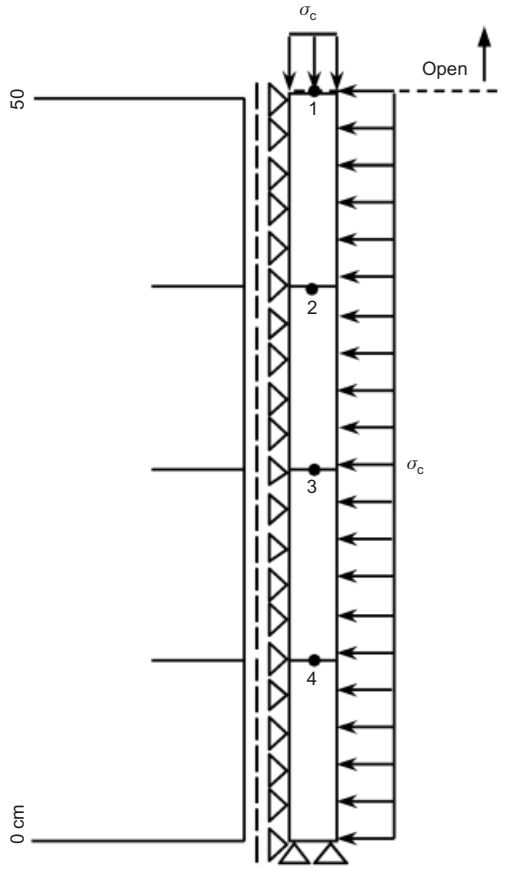

Fig. 11. Axisymmetric FE model of triaxial specimen

an insignificant part of the total time, then all deformation–time curves of the sub-specimens converge to the same point.

The deformation characteristics of different soil elements within one thick specimen are analogous to the deformation behaviour observed in specimens of different thickness, except that in the first case there is one EOP time defined for the whole sample, whereas in the latter case there are different EOP times for the respective thicknesses. The implication of isotaches, for soil elements located at different distances from the drainage boundary (Fig. 11), can be elaborated by considering the interplay between creep rate and the time for which the applied effective stress is sustained (the 'effective creep time'). Even though there is only one EOP time considered for the entire specimen, the sub-specimen that is closest to the drainage boundary (the top sub-specimen) sustains the applied effective stress for a longer time than the sub-specimen located farthest from the drainage boundary (the bottom sub-specimen). This is because consolidation is completed instantaneously at the open drainage boundary and the top sub-specimen immediately continues to the secondary consolidation phase whereas the bottom sub-specimen experiences only the primary consolidation phase. Hence the top sub-specimen has a longer effective creep time than the bottom sub-specimen.

Before exceeding the initial p'_c, all the sub-specimens start at a similar creep rate; however, during an effective stress increment that exceeds the initial p'_c, the effective creep time is different for each sub-specimen, and this leads to different sub-specimen EOP strains. As a result, the sub-specimens closer to the drainage boundary experiences higher EOP strain than the sub-specimens located farther from the drainage boundary. After exceeding the initial p'_c, the top and bottom sub-specimens no longer start at similar

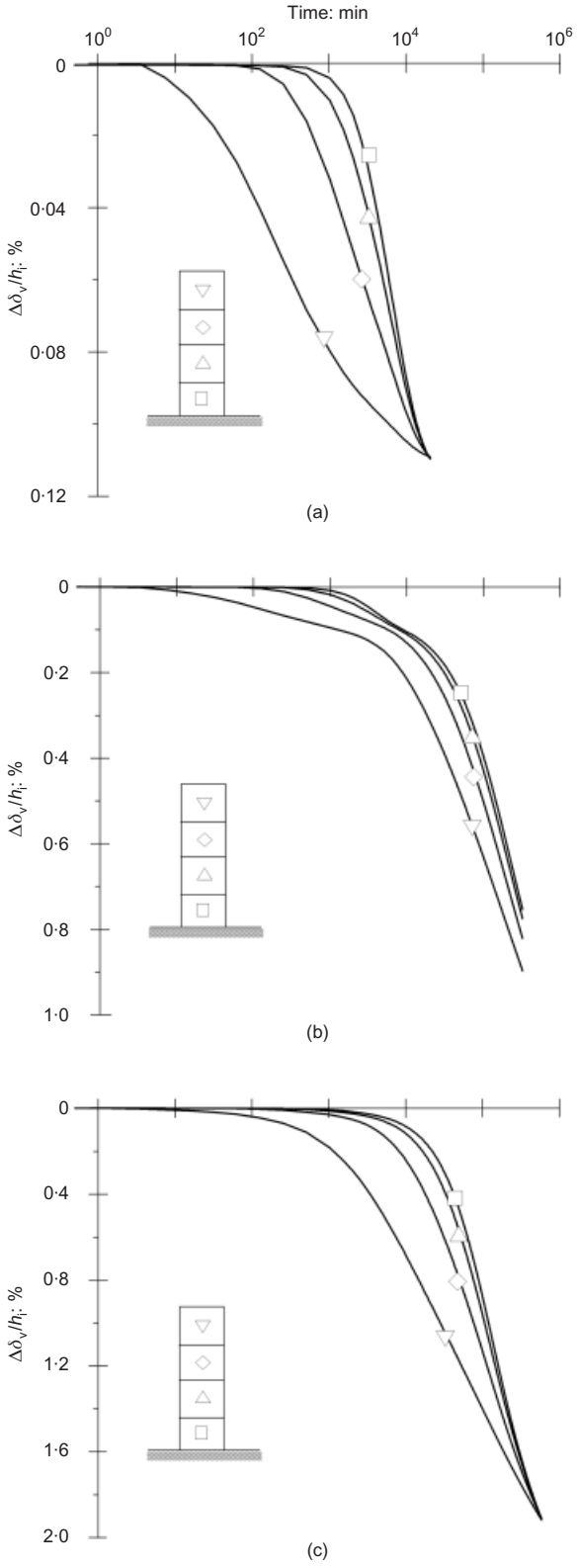

Fig. 12. Incremental nominal strains at different points within one thick specimen with reference to initial p'_c (after Feng, 1991): (a) before exceeding initial p'_c; (b) exceeding initial p'_c; (c) after exceeding initial p'_c

creep rates, as the top sub-specimen has a lower creep rate than the bottom sub-specimen. Hence, for stress increments in the normally consolidated regime, the top sub-specimen deforms with a lower creep rate for a longer effective creep time, whereas the bottom sub-specimen deforms with a higher creep rate for a shorter effective creep time. As a

result, the incremental sub-specimen EOP strains, in the normally consolidated regime, will be practically the same for all sub-specimens.

Experiment by Feng (1991)

Feng (1991) conducted experimental investigations of natural soft clays that included EOP tests of high-quality block samples on Batiscan and St-Hilaire clays. Specimens with an initial thickness of 508 mm and a diameter of 63·5 mm were tested from each of the two clay samples. The 508 mm thick specimen was obtained by interconnecting four 127 mm thick sub-specimens in series. The tests were conducted in triaxial cells with an isotropic incremental loading scheme and one-way drainage condition. The triaxial apparatus was preferred to avoid problems related to side friction that exist in an oedometer cell. Each isotropic load increment was maintained until the final excess pore pressure was approximately 1 kPa. The data acquisition method was primarily based on the total volume change reading of a burette and an axial compression device mounted on the top of each specimen. Similar tests have also been conducted by Choi (1982) on San Francisco Bay Mud and Saint-Alban clay. However, the tests conducted by Feng (1991) are preferred for this illustration, by the virtue of the fact that there exists additional information on the axial compression of each sub-specimen during the test.

The incremental loading sequence for Batiscan clay was 14, 28, 41, 62, 83 and 138 kPa, and for St-Hilaire clay it was 34, 62, 97 and 138 kPa. From the 508 mm thick specimen tests, Feng (1991) estimated the value of the initial preconsolidation stress to be 52 kPa for Batiscan and 76 kPa for St-Hilaire clay.

The compressibility of the clay specimen in the triaxial stress state is preferably studied using the volumetric strains. However, since the volume of water expelled from the individual sub-specimens was not measured during the test, the axial compressions of the individual sub-specimen were studied instead. Such information will equally provide the general trend of the deformation characteristics of the soil elements. The incremental axial nominal strains within each sub-specimen are presented, in Fig. 13, for the three different stress regimes with reference to the initial p'_c.

Feng (1991) was interested in studying the local (sub-specimen) void ratio change within the 508 mm thick specimen in order to investigate the time and stress compressibility of the clays. To do this, the local void ratios had to be interpreted based on the total volume change and four local axial compression measurements. Hence the measured total volume change was distributed among the four sub-specimens using two different approaches, which are described in detail by Feng (1991: 549–554). Feng referred to the two procedures as approach A and approach B. Approach A was used for the stress increments before and after the stress exceeded the initial p'_c, and approach B was used for the stress increment that exceeded the initial p'_c. In approach A, the volumetric deformations were scaled proportionally based on the axial deformations. This resulted in volume–time relationships of the sub-specimens that essentially became analogous to the axial compression–time plot, where the local change in nominal strain at the EOP is identical for all sub-specimens. Hence approach A yielded local volume (void ratio) changes that were unique for all sub-specimens, and Feng considered these interpreted results to be in line with creep hypothesis A. However, Feng opted to use approach B for stress increments that exceeded the initial p'_c. Based on the time–axial compression measurements of the stress increments that spanned the initial p'_c (Fig. 13), Feng argued that 'approach A cannot be used for this increment, since these axial compression curves do not merge with each other at the end of primary consolidation. Therefore a different approach is required.' In other words, if approach A had been used for the stress increment that exceeded the initial p'_c, then the interpreted local void ratio changes would not have been unique for the sub-specimens. In approach B the local volumetric changes are directly calculated assuming the validity of creep hypothesis A. In this way, the local volume change–time plots of the four sub-specimens were 'adjusted' to come to the same point at the EOP state. It should, however, be acknowledged that the measured volumetric changes were considerably larger than the axial compression during this step (i.e. significantly larger horizontal strain than axial strain). The reason for this special behaviour is assumed to be that the soil first started to yield in the horizontal direction before yielding in the axial direction, which means that the horizontal preconsolidation stress was lower than the vertical preconsolidation stress (typical anisotropic behaviour can be found in normally consolidated clay; e.g. Leroueil, 2006). It is, though, still difficult to understand why Feng opted to use a significantly different ratio of horizontal to axial strain, in the different sub-specimens, for the load step that exceeded the initial p'_c. The 'adjusted' results were later presented as 'experimental evidence' showing a unique EOP void ratio for soil elements located within the thick specimen (Feng 1991; Mesri *et al.*, 1994; Mesri, 2003). It is important to note that this 'adjustment' affected all interpreted results that come after exceeding the initial p'_c. Other researchers (Leroueil *et al.*, 1986; Leroueil, 1996, 2006; Leroueil & Marques, 1996) have previously suggested that the reason why the interpreted local void ratio of the sub-specimens of the St-Hilaire clay, for the stress increment of 97–138 kPa (after exceeding the initial p'_c), seemed unique could be due to 'uniformisation' of the strain rate at the EOP state. However, this study has shown that for all the stress increments, starting from the step that exceeds the initial p'_c, there is no 'uniformisation' of strain rate at EOP. It only seemed uniform because the results were reset, and the information on the sub-specimen isotaches was hidden. It is clear that it is only the incremental axial compression–time curves that converge to the same point for the stress increment after the initial p'_c; otherwise, the absolute axial compression curves will maintain their differences, which arose while exceeding the initial p'_c.

The trends of the experimental results of both Batiscan and St-Hilaire clays (Fig. 13) are in complete agreement with the isotache concept as illustrated in the idealised case II (Fig. 12). In all cases the axial deformations are presented in terms of the change in nominal strain. These curves start and end at the same point for stress increments before and after the initial p'_c, but will never come to the same point for the stress increment that exceeds the initial p'_c. In fact, the results of idealised case II, which were simulated using representative parameters of Batiscan clay, show very good agreement with the experimental observations shown in Fig. 13(a), (c) and (e).

CONCLUSIONS

With regard to the effect of creep during primary consolidation, two extreme cases, named creep hypotheses A and B, have been used as a basis of discussion. Various laboratory data as well as field observations have been presented in the literature that seem to support either of the two hypotheses. Therefore the main motivation of this work was to explain, in a consistent manner, laboratory test results relevant to the two creep hypotheses. As a result, selected test results are thoroughly studied and critically assessed.

In response to the important question raised by Ladd *et*

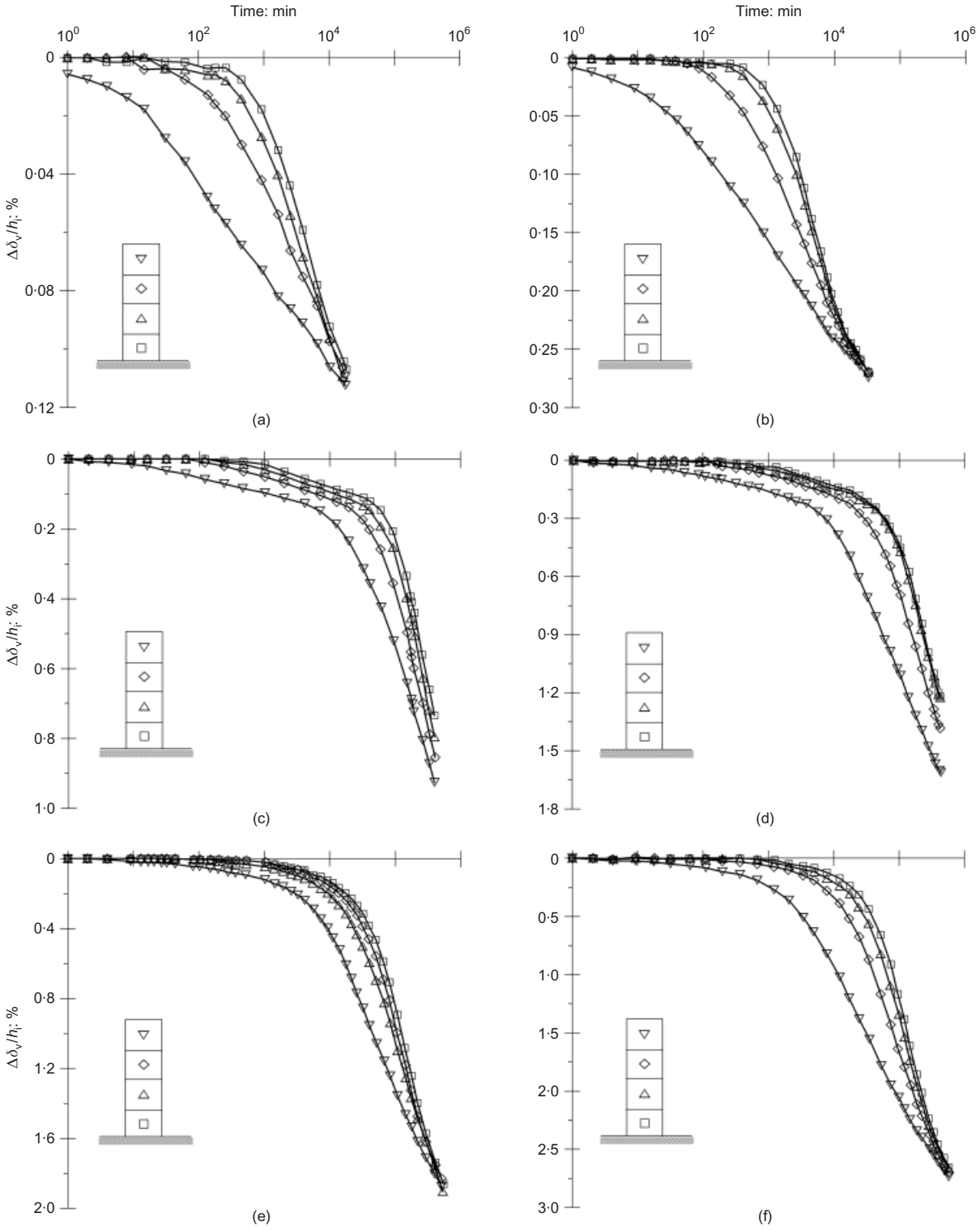

Fig. 13. Incremental sub-specimen nominal strains against time: before exceeding initial p'_c for (a) Batiscan clay, 28–41 kPa, (b) St-Hilaire clay, 34–62 kPa; exceeding initial p'_c for (c) Batiscan clay, 41–62 kPa, (d) St-Hilaire clay, 62–97 kPa; after exceeding initial p'_c for (e) Batiscan clay, 62–83 kPa, (f) St-Hilaire clay, 97–138 kPa (after Feng, 1991)

al. (1977), this study has shown that there exist definitive data to demonstrate that hypothesis B agrees very well with the measured behaviour of cohesive soils. Experimental observations that were previously used to claim hypothesis A have herein been explained consistently using a model based on the isotache concept.

It is only when considering the incremental strain (change in void ratio), during stress increment in the normally consolidated regime, that there seems to be a unique EOP strain (void ratio) for both the thin and the thick specimens. However, this is not valid for a general stress history. With this aspect, this work has demonstrated that hypothesis A is wrong for stress increments that exceed the initial preconsolidation stress, as well as for stress increments even in the normally consolidated regime when the whole effective stress–strain (void ratio) history is considered. This study has also shown that results that have been used to validate hypothesis A have been presented misleadingly, and in one case also adjusted inconsistently.

An important observation from this study is that the compressibility of clay must be studied taking into account the effect of previous stress history. For single load increment tests it is important to keep track of the starting void ratio, along with the corresponding preconsolidation stress.

Future developments related to the compressibility of natural clays should be focused on enhancing models that are based on the isotache framework. Parts of the important extensions include modelling anisotropy and structure/destructuration effects.

ACKNOWLEDGEMENTS

The work described in this paper is supported by the Research Council of Norway through the International Centre for Geohazards (ICG). Their support is gratefully acknowledged. This is ICG contribution No. 302.

Researchers whose works have been discussed in this paper are greatly acknowledged and appreciated for providing high-quality test results that made this study possible.

REFERENCES

Aboshi, H. (1973). An experimental investigation on the similitude in the consolidation of a soft clay, including the secondary creep settlement. *Proc. 8th Int. Conf. Soil Mech. Found. Engng, Moscow* **4**, No. 3, 88.

Aboshi, H., Matsuda, H. & Okuda, M. (1981). Preconsolidation by separate-type consolidometer. *Proc. 10th Int. Conf. Soil Mech. Found. Engng, Stockholm* **3**, 577–580.

Berre, T. & Iversen, K. (1972). Oedometer tests with different specimen heights on a clay exhibiting large secondary compression. *Géotechnique* **22**, No. 1, 53–70, **doi**: 10.1680/geot.1972.22.1.53.

Bjerrum, L. (1967). Engineering geology of Norwegian normally consolidated marine clays as related to settlements of buildings. *Géotechnique* **17**, No. 2, 81–118, **doi**: 10.1680/geot.1967.17.2.81.

Chih-Hao, T. (2002). *The behavior of compression and consolidation for clays* (in Chinese). PhD thesis, National Central University, Taiwan.

Choi, Y. K. (1982). *Consolidation behavior of natural clays*. PhD thesis, University of Illinois at Urbana-Champaign, Urbana-Illinois.

Degago, S. A., Grimstad, G., Jostad, H. P. & Nordal, S. (2009). The non-uniqueness of the end-of-primary (EOP) void ratio-effective stress relationship. *Proc. 17th Int. Conf. Soil Mech. Geotech. Engng, Alexandria* **1**, 324–327.

Degago, S. A., Jostad, H. P., Olsson, M., Grimstad, G. & Nordal, S. (2010). Time- and stress-compressibility of clays during primary consolidation. *Proc. 7th Eur. Conf. Numer. Methods Geotech. Engng, Trondheim*, 125–130.

Den Haan, E. J. (1996). A compression model for non-brittle soft clays and peat. *Géotechnique* **46**, No. 1, 1–16, **doi**: 10.1680/geot.1996.46.1.1.

Feng, T. W. (1991). *Compressibility and permeability of natural soft clays and surcharging to reduce settlements*. PhD thesis, University of Illinois at Urbana-Champaign, Urbana-Illinois.

Felix, B. (1979). *Fluage et consolidation undimensionnels des sols argileux*. PhD thesis, DI Paris VI (in French).

Grimstad, G. & Degago, S.A. (2010). A non-associated creep model for structured anisotropic clay (n-SAC). *Proc. 7th Eur. Conf. Numer. Methods Geotech. Engng, Trondheim*, 3–8.

Grimstad, G., Degago, S. A., Nordal, S. & Karstunen, M. (2010). Modeling creep and rate effects in structured anisotropic soft clays. *Acta Geotech*. **5**, No. 1, 69–81.

Hawlader, B. C., Muhunthan, B. & Imai, G. (2003). Viscosity effects on one-dimensional consolidation of clay. *ASCE Int. J. Geomech*. **3**, No. 1, 99–110.

Imai, G. & Tang, Y. X. (1992). Constitutive equation of one-dimensional consolidation derived from inter-connected tests. *Soils Found*. **32**, No. 2, 83–96.

Imai, G., Tanaka, Y. & Saegusa, H. (2003). One-dimensional consolidation modeling based on the isotache law for normally consolidated clays. *Soils Found*. **43**, No. 4, 173–188.

Janbu, N. (1969). The resistance concept applied to deformations of soils. *Proc. 7th Int. Conf. Soil Mech. Found. Engng, Mexico City* **1**, 191–196.

Kabbaj, M., Tavenas, F. & Leroueil, S. (1988). In situ and laboratory stress–strain relations. *Géotechnique* **38**, No. 1, 83–100, **doi**: 10.1680/geot.1988.38.1.83.

Karim, M. R., Gnanendran, C. T., Lo, S.-C. R. & Mak, J. (2010). Predicting the long term performance of a wide embankment on soft soil using an elastic-viscoplastic model. *Can. Geotech. J.* **47**, No. 2, 244–257.

Kim, Y. T. & Leroueil, S. (2001). Modeling the viscoplastic behavior of clays during consolidation: application to Berthierville clay in both laboratory and field conditions. *Can. Geotech. J.* **38**, No. 3, 484–497.

Konovalov, P. A. & Bezvolev, S. G. (2005). Analysis of results of consolidation tests of saturated clayey soils. *Soil Mech. Found. Engng* **42**, No. 3, 81–85.

Kutter, B. L. & Sathialingam, N. (1992). Elastic-viscoplastic modelling of the rate-dependent behaviour of clays. *Géotechnique* **42**, No. 3, 427–442, **doi**: 10.1680/geot.1992.42.3.427.

Ladd, C. C., Foott, R., Ishihara, K., Schlosser, F. & Poulos, H. G. (1977). Stress-deformation and strength characteristics. state-of-the-art report. *Proc. 9th Int. Conf. Soil Mech. Found. Engng, Tokyo* **2**, 421–494.

Laloui, L., Leroueil, S. & Chalindar, S. (2008). Modeling the combined effect of strain rate and temperature on one-dimensional compression of soils. *Can. Geotech. J.* **45**, No. 12, 1765–1777.

Larsson, R. & Mattsson, H. (2003). *Settlements and shear strength increase below embankments*, Report 63. Linköping: Swedish Geotechnical Institute.

Leoni, M., Karstunen, M. & Vermeer, P. A. (2008). Anisotropic creep model for soft soils. *Géotechnique* **58**, No. 3, 215–226, **doi**: 10.1680/geot.2008.58.3.215.

Leroueil, S. (1996). Compressibility of clays: fundamental and practical aspects. *ASCE J. Geotech. Engng Div.* **122**, No. 7, 534–543.

Leroueil, S. (2006). Šuklje Memorial Lecture: The isotache approach. Where are we 50 years after its development by Professor Šuklje? *Proc. 13th Danube Eur. Conf. Geotech. Engng, Ljubljana* **2**, 55–88.

Leroueil, S. & Marques, M. E. S. (1996). Importance of strain rate and temperature effects in geotechnical engineering. In *Measuring and modeling time dependent soil behaviour* (eds T. C. Sheahan and V. N. Kaliakin), Geotechnical Special Publication 61, pp. 1–60. New York: ASCE

Leroueil, S., Kabbaj, M., Tavenas, F. & Bouchard, R. (1985). Stress–strain–strain rate relation for the compressibility of sensitive natural clays. *Géotechnique* **35**, No. 2, 159–180, **doi**: 10.1680/geot.1985.35.2.159.

Leroueil, S., Kabbaj, M., Tavenas, F. & Bouchard, R. (1986). Closure of 'Stress–strain–strain rate relation for the compressibility of sensitive natural clays' by Leroueil, Kabbaj, Tavenas & Bouchard (1985). *Géotechnique* **36**, No. 2, 288–290, **doi**: 10.1680/geot.1986.36.2.288.

Li, S., Shirako, H., Sugiyama, M. & Akaishi, M. (2004). Time effects on one-dimensional consolidation analysis. *Proc. Schl. Eng. Tokai Univ. Ser. E* **29**, 1–8.

Mesri, G. (1990). Discussion of 'Viscous-elastic-plastic modeling of one-dimensional time-dependent behavior of clays' by Yin & Graham (1989). *Can. Geotech. J.* **27**, No. 2, 259–261.

Mesri, G. (2003). Primary and secondary compression. In *Soil behavior and soft ground construction* (eds J. T. Germaine, T. C. Sheahan and R. V. Whitman), Geotechnical Special Publication 119, pp. 122–166. Reston, VA: ASCE.

Mesri, G. (2009). Discussion of 'Effects of friction and thickness on long-term consolidation behavior of Osaka Bay clays' by Watabe, Udaka, Kobayashi, Tabata & Emura (2008). *Soils Found*. **49**, No. 5, 823–824.

Mesri, G. & Choi, Y. K. (1985). The uniqueness of the end-of-primary (EOP) void ratio-effective stress relationship. *Proc. 11th Int. Conf. Soil Mech. Found. Engng, San Francisco* **2**, 587–590.

Mesri, G. & Godlewski, P. M. (1979). Closure of 'Time and stress-

compressibility interrelationship' by G. Mesri & P. M. Godlewski (1977). *ASCE J. Soil Mech. Found. Div.* **105**, No. GT1, 106–113.

Mesri, G. & Vardhanabhuti, B. (2006). Closure of 'Secondary compression' by Mesri & Vardhanabhuti (2005). *J. Geotech. Geoenviron. Engng* **132**, No. 6, 817–818.

Mesri, G., Lo, D. O. K. & Feng, T. W. (1994). Settlements of embankments on soft clays. *Proceedings of Settlement '94: Vertical and Horizontal Deformations of Foundations and Embankments, College Station, TX* **1**, 8–56.

Mesri, G., Feng, T. W. & Shahien, M. (1995). Compressibility parameters during primary consolidation. *Proceedings of the international symposium on compression and consolidation of clayey soils*, Hiroshima, Vol. 2, pp. 1021–1037.

Nash, D. F. T. (2010). Influence of destructuration of soft clay on time-dependent settlements. *Proc. 7th Eur. Conf. Numer. Methods Geotech. Engng, Trondheim*, 75–80.

Nash, D. F. T. & Ryde, S.J. (2001). Modelling the consolidation of compressible soils subject to creep around vertical drains. *Géotechnique* **51**, No. 4, 257–273, **doi**: 10.1680/geot.2001.51.4.257.

Oka, F. (2005). Computational modelling of large deformations and the failure of geomaterials. Theme lecture. *Proc. 16th Int. Conf. Soil Mech. Geotech. Engng, Osaka* **1**, 47–95.

Oka, F., Adachi, T. & Okano, Y. (1986). Two-dimensional consolidation analysis using an elasto-viscoplastic constitutive equation. *Int. J. Numer. Anal. Methods Geomech*. **10**, No. 1, 1–16.

Stolle, D. F. E., Vermeer, P. A. & Bonnier, P. G. (1999). Consolidation model for a creeping clay. *Can. Geotech. J.* **36**, No. 4, 754–759.

Šuklje, L. (1957). The analysis of the consolidation process by the isotaches method. *Proc. 4th Int. Conf. Soil Mech. Found. Engng, London* **1**, 200–206.

Šuklje, L. (1969). *Rheological aspects of soil mechanics*. London: John Wiley & Sons.

Svanø, G., Christensen, S. & Nordal, S. (1991). A soil model for consolidation and creep. *Proc. 10th Int. Conf. Soil Mech. Found. Engng, Florence* **1**, 269–272.

Tanaka, H. (2005). Consolidation behaviour of natural soils around p_c value-inter-connected oedometer test. *Soils Found*. **45**, No. 3, 97–105.

Tsukada, Y. & Yasuhara, K. (1995). Scale effects in one-dimensional consolidation of clay. *Proceedings of the international symposium on compression and consolidation of clayey soils*, Hiroshima, pp. 211–216.

Vermeer, P. A. & Neher, H. P. (1999). A soft soil model that accounts for creep. In *Beyond 2000 in computational geotechnics: 10 Years of Plaxis* International (ed. R. B. J. Brinkgreve), pp. 249–261. Rotterdam: Balkema

Watabe, Y., Udaka, K., Kobayashi, M., Tabata, T. & Emura, T. (2008a). Effects of friction and thickness on long-term consolidation behavior of Osaka Bay clays. *Soils Found*. **48**, No. 4, 547–561.

Watabe, Y., Udaka, K. & Morikawa, Y. (2008b). Strain rate effect on long-term consolidation of Osaka Bay clay. *Soils Found*. **48**, No. 4, 495–509.

Watabe, Y., Tanaka, M., Sassa, S., Kobayashi, M. & Udaka, K. (2009). Effects of specimen thickness and skeletal structure on consolidation behavior around yield stress. *Proc. 17th Int. Conf. Soil Mech. Geotech. Engng, Alexandria* **1**, 696–699.

Yasuhara, K. (1982). A practical model for secondary compression. *Soils Found*. **22**, No. 4, 45–56.

Yin, J. -H., Zhu, J. G. & Graham, J. (2002). A new elastic-viscoplastic model for time-dependent behavior of normally and over consolidated clays: Theory and verification. *Can. Geotech. J.* **39**, No. 1, 157–173.